

## Discovering the potential of natural remedies in the post COVID-19 complications based on in silico techniques

Alkeshkumar Patel <sup>\*</sup>, Ashish Patel , Rushikumar Shah ,  
Diwyanshi Zinzuvadia  and Sagar Mahant 

Dept. of Pharmacology, Ramanbhai Patel college of Pharmacy, CHARUSAT, Gujarat, India

(Received February 17, 2022; Revised April 23, 2022; Accepted April 29, 2022)

**Abstract:** The first incidence of corona virus was reported in China in December of 2019, and the virus quickly spread over the world, eventually being designated a pandemic in March of 2020. It has had a disastrous impact on the global healthcare system. Virus has claimed the lives of 5,298,933 people through December 2021. As a result of the pandemic, there was a boost of research into diagnostic and therapeutic methods to infection. Gradually, the world has discovered new vaccine candidates and medicinal repurposing strategies that have a significant influence on mortality, by which there has been a drop-in death rates over the world since July, 2021. Many patients, particularly those who have been hospitalized due to a viral infection, experience complications beyond discharge that have a significant influence on their lives. Post COVID-19 complications are problems that last longer than 3-4 weeks following a viral infection. There is currently no specific treatment accessible for post COVID-19 problems because whatever medications are available or repurposed are limited to disease prophylaxis and therapeutics. As a result, we're looking for a remedy employing natural substances using the In-Silico technique (molecular docking) and recent research from reputable journals. Allicin, Berberine, Epigallocatechin, Rosmarinic acid and Withaferin-A were docked against ACE (PDB ID: 1O8A), IL-6 (PDB ID: 1ALU), NADPH Oxidase (PDB ID: 2CDU) and TNF- $\alpha$  (PDB ID: 2AZ5) using Autodock.

**Keywords:** Natural remedies; post COVID-19; hyper inflammation; cytokine storm; Autodock. ©2022. ACG Publications. All right reserved.

### 1. Introduction

China has reported multifold cases of viral pneumonia in Wuhan city during December 2019. Later, it was discovered that Coronavirus causes such condition and termed as 2019-nCoV (2019- novel coronavirus) which generally transfers from human to human and have been spread worldwide.<sup>1</sup> COVID-19 is found to be the third zoonotic disease to affect humans following SARS and MERS. Coronaviruses are single-stranded RNA viruses that cause upper and lower respiratory tract infections.<sup>2</sup> To enter the host cell, spike glycoproteins present in the structure of the coronaviruses bind to angiotensin-converting enzyme-2 (ACE-2) present in the lungs.<sup>3</sup> Routes of transmission of COVID-19 are through cough, sneezing, oral, and nasal and eye mucous membranes.<sup>4</sup> During COVID-19 infection, patients experience varieties of signs and symptoms like dyspnea, chills, cold, dry cough and hypoxia in the systemic circulation. These are indications of primary stages where the body's immune system tries to restrict the progress of the disease. As the disease progresses it may lead to hyper inflammation due to cytokine storm, coagulopathy, organs (kidney, liver, lung, heart) failure, rise in C-reactive protein, lactate dehydrogenase along with D-dimer while the collapse in lymphocyte count.

WHO has reported five variants of COVID-19 till December, 2021 – (I) Alpha-B.1.1.7: First reported in the UK in late December 2020 (II) Beta-B.1.351: First reported in South Africa in December

\* Corresponding author: E-Mail: [alkeshpatel.ph@charusat.ac.in](mailto:alkeshpatel.ph@charusat.ac.in) ; Phone: + 91 9978986530

The article was published by ACG Publications

<http://www.acgpubs.org/journal/organic-communications> © April-June 2022 EISSN:1307-6175

DOI: <http://doi.org/10.25135/acg.oc.128.2202.2356>

Available online: May 21, 2022

2020 (III) Gamma-P.1: First reported in Brazil in early January 2021 (IV) Delta-B.1.617.2: First reported in India in December 2020 (V) Omicron (B.1.1.529): First reported in South Africa in November 2021.<sup>5,6</sup> Mostly COVID-19 patients are observed asymptomatic as compared to symptomatic. Diagnosis of COVID-19 is performed by various tests such as real-time PCR assay, serology test, complete blood count (CBC), chest X-ray, chest compound tomography (CT), lung ultrasound, Test for inflammatory marker such as C-reactive protein (CRP), ferritin, D-dimer and lactate dehydrogenase. Current therapeutic approaches for COVID-19 include antimalarial agents such as chloroquine and hydroxychloroquine, antiviral agents such as remdesivir, lopinavir-ritonavir, and arbidol, Interleukin-6 (IL-6) receptor antagonists, NSAIDs, bronchodilators or vasodilators, mechanical ventilation, and vaccines.<sup>7</sup>

Around the world, numerous vaccines are under trial in various countries.<sup>8</sup> Development of vaccines includes strategies such as whole inactivated virus, live attenuated virus, protein subunit, virus-like particle, viral vector, antigen-presenting cells, DNA, and RNA.<sup>9</sup> Vaccines developed for COVID-19 are AstraZeneca/ChAdOx1 nCoV-19 (nonreplicating chimpanzee viral vector vaccine) developed by the University of Oxford and the British-Swedish pharmaceutical company AstraZeneca, COVAXIN (inactivated coronavirus) developed by Bharat Biotech in collaboration with Indian Council of Medical Research (ICMR) and National Institute of Virology (NIV), mRNA-1273 (mRNA encoding a stabilized S protein is encapsulated in lipid nanoparticles) developed by Moderna, BNT162b2 (lipid nanoparticle (LNP)-encapsulated, nucleoside-modified mRNA) developed by Pfizer, Sputnik V (two non-replicating viral vectors, adenovirus type 5 (rAd5) and adenovirus type 26 (rAd26)) developed by Gamaleya research institute and Ad26.CoV2.S (a non-replicating, adenovirus type 26 (Ad26)-vector) developed by Janssen pharmaceutical.<sup>10,11</sup>

Post COVID-19 can be defined as the persistence of symptoms beyond 3 to 4 weeks from the onset of acute symptoms of COVID-19.<sup>12</sup> Post COVID-19 can also be denoted as persistence of signs and symptoms after viral clearance, development of symptoms after recovery from COVID-19 infection, amplification in previously experienced chronic disease after recovery from COVID-19.<sup>13</sup> It includes consequences in various parts of the body such as pulmonary, hematologic, cardiovascular, kidney damage, neuropsychiatric, renal, endocrine, gastrointestinal and dermatologic.<sup>12</sup> Most commonly observed post COVID-19 symptoms are fatigue, chest pain, chronic inflammation, struggling for breath, hepatic damage, cardiovascular damage, slight fever, joint pain, and headache. The majority of problems are due to chronic inflammation and oxidative stress. There is no proven remedy or treatment drug to alleviate post COVID-19 symptoms.<sup>13</sup>

### *1.1. Understanding Post COVID-19 Pathology and Pathophysiology*

Most of the COVID-19 patients recover within 2-4 weeks if they get proper treatment in the hospital and live complications-free life. Although few patients suffer post COVID-19 complications and show symptoms even after recovery even RT-PCR shows negative results. This condition is represented as post COVID-19 syndrome. According to the National Institute for Health and Care Excellence (NICE), the post COVID-19 syndrome is confirmed if signs and symptoms develop during or after an infection consistent with COVID-19, continuing for more than 12 weeks (3 months), and not explained by an alternative diagnosis.

It involves a wide range of symptoms like fever, organ (kidney, liver, heart) damage that may lead to its failure, coagulopathy,<sup>14</sup> fatigue, impaired memory, mood disorders, joints pains, cardiac myocyte damage, insomnia, dyspnea due to alveolar damage, arrhythmias, telogen effluvium, multisystem inflammatory syndrome,<sup>15</sup> development of diabetes mellitus due to pancreatic  $\beta$ -cell infection followed by necrosis or get reprogrammed by transdifferentiation.<sup>16</sup> Much evidence shows the development of brain disorders like Guillain-Barre syndrome, encephalitis, seizures, and strokes. These symptoms majorly belong to the cardiopulmonary, urinary, endocrine, and nervous systems. Although the involvement of the gastrointestinal and reproductive system cannot be neglected.<sup>17</sup> Even excessive oxidative stress leads to neurodegeneration and increases the risk of Parkinson's and Alzheimer's disease occurrences.

Based on the prevalence of cell death in tissue, particular symptoms may appear from 3-6 months.<sup>12</sup> The residual effects of post COVID-19 syndrome may be due to an overwhelming response

## Discovering the potential of natural remedies in the post COVID-19 complications

of innate immunity that damages multiple tissue cells. The dysregulated immune activation triggers hyper inflammation, cytokines secretion with pro-coagulation situations in the body.<sup>18</sup> There are multiple pathophysiologic processes reported by different researchers that include COVID-19 mediated activation of abnormal immune and inflammatory signalling pathways, an aberration in Renin angiotensin aldosterone system, abnormal thrombus formation in macro-and microcirculation due to elevated D-dimer and fibrinogen values, changes in bioenergetics of the host cell that shift energy-yielding process from oxidative phosphorylation to glycolysis.

### *1.2. Need of Natural Remedies to Rejuvenate Collapsed Host System*

The available therapeutic options work limited against post COVID-19 syndrome. Also, there are possibilities of side effects and toxicities as concerns of long-term application. So, we selected the best natural revitalizers from the Indian traditional system that work in diverse abnormal pathophysiology of post COVID-19 and improve the quality of COVID-19 infected patients. In such a situation, people mostly rely on nutraceuticals such as immunity-boosting foods, drinks, and supplements to escalate the recovery phase.<sup>19</sup> More commonly, Vitamin C and Zinc have emerged as strong COVID-19 fighters since a lot of people believed that the two nutrients work to supercharge immunity thereby used by post COVID-19 symptomatic patients also.<sup>20,21</sup> Supporting this notion, we have chosen four natural plants and their constituents that are responsible for their effect. It includes Ashwagandha, Berberine, Green tea, Rosmarinic acid, and *Allium sativum*. This herbal acts as an immunomodulator, therapeutic adjuvant, and fighting post COVID-19 effects.

Ashwagandha is used widely in numerous disease conditions. In the case of post COVID-19 symptoms, there are pre-clinical results that confirm its anti-inflammatory, antioxidant, antiviral, immunomodulatory, and cytoprotective effect.<sup>22-25</sup> Clinical trials have proven that Ashwagandha exhibits cardiorespiratory protective agents and hepatoprotective agents.<sup>22</sup> Berberine is a natural isoquinoline alkaloid with various protective effects that helps in post COVID-19 management.<sup>26</sup> Berberine along with obatoclax is found to exhibit inhibition of SARS-Cov-2 replication in primary human nasal epithelium cells in vitro.<sup>27</sup> Green tea contains epigallocatechin gallate (EGCG) phenolic catechin that shows the antiviral activity as a potential treatment option against synthetic drugs.<sup>28</sup> Catechin shows various effects that include antioxidant, anti-inflammatory, antimutagenic, antimicrobial, and antiviral and immunomodulatory activities.<sup>29</sup>

Rosmarinic acid found in various herbal plants is a polyphenolic antioxidant that has proven to exhibit positive effects against hepatic reperfusion injury.<sup>30</sup> It is also found that rosmarinic acid acts by inhibiting the angiotensin-converting enzyme in hypertensive models of animals.<sup>31</sup> Along with the above two effects of rosmarinic acid, it also shows effects similar to Ashwagandha and berberine.<sup>32,33</sup> *Allium sativum* (garlic) has exhibited many effects that are potential to influence immunity. Allicin a phytoconstituent present in garlic shows the effect to decrease the expression of proinflammatory cytokines that are responsible for cytokine storm in COVID-19 patients. *Allium sativum* has shown positive effects in blood coagulation and can treat complications related to the nervous, reproductive, and endocrine systems.<sup>34</sup>

Because herbal plants come from a variety of families, including Solanaceae, Berberidaceae, Theaceae, Lamiaceae, and Amaryllidaceae, the structure of each phytoconstituent varies. Phytoconstituents are found in abundance in all herbal plants. Some of the active phytoconstituents have demonstrated positive outcomes in various pre-clinical and clinical investigations against the specified targets, out of all the active phytoconstituents. The phytoconstituents withaferin A from Ashwagandha, Berberine, a natural isoquinoline alkaloid, Epigallocatechin from green tea, Rosmarinic acid, and Allicin from *Allium sativum* were chosen for the In-silico investigations based on the literature survey.

All the five herbal plants and phytoconstituents show almost similar effects so our objective is to test our formulation in silico, in vitro, or in vivo. Our targets include ACE (Angiotensin-converting enzyme), Interleukin-6 (IL-6), TNF-alpha, and NADPH oxidase. ACE is one of the main enzymes of the renin-angiotensin system. ACE converts angiotensin I (AngI) to angiotensin II (AngII). AngII is responsible for increased levels of reactive oxygen species (ROS) and superoxide levels which are responsible for oxidative stress.<sup>35</sup> AngII is also responsible for high blood pressure because it causes vasoconstriction in blood vessels.<sup>36</sup> SOD is an enzyme that works by breaking down harmful oxygen

species which are responsible for oxidative stress.<sup>37</sup> During COVID-19 infection, the level of SOD is decreased which leads to an imbalance between reactive oxygen species.<sup>38</sup> TNF-alpha and IL-6 are a cytokines that plays a crucial role in COVID-19 patients and is also responsible for the severity of the infection.<sup>39</sup>

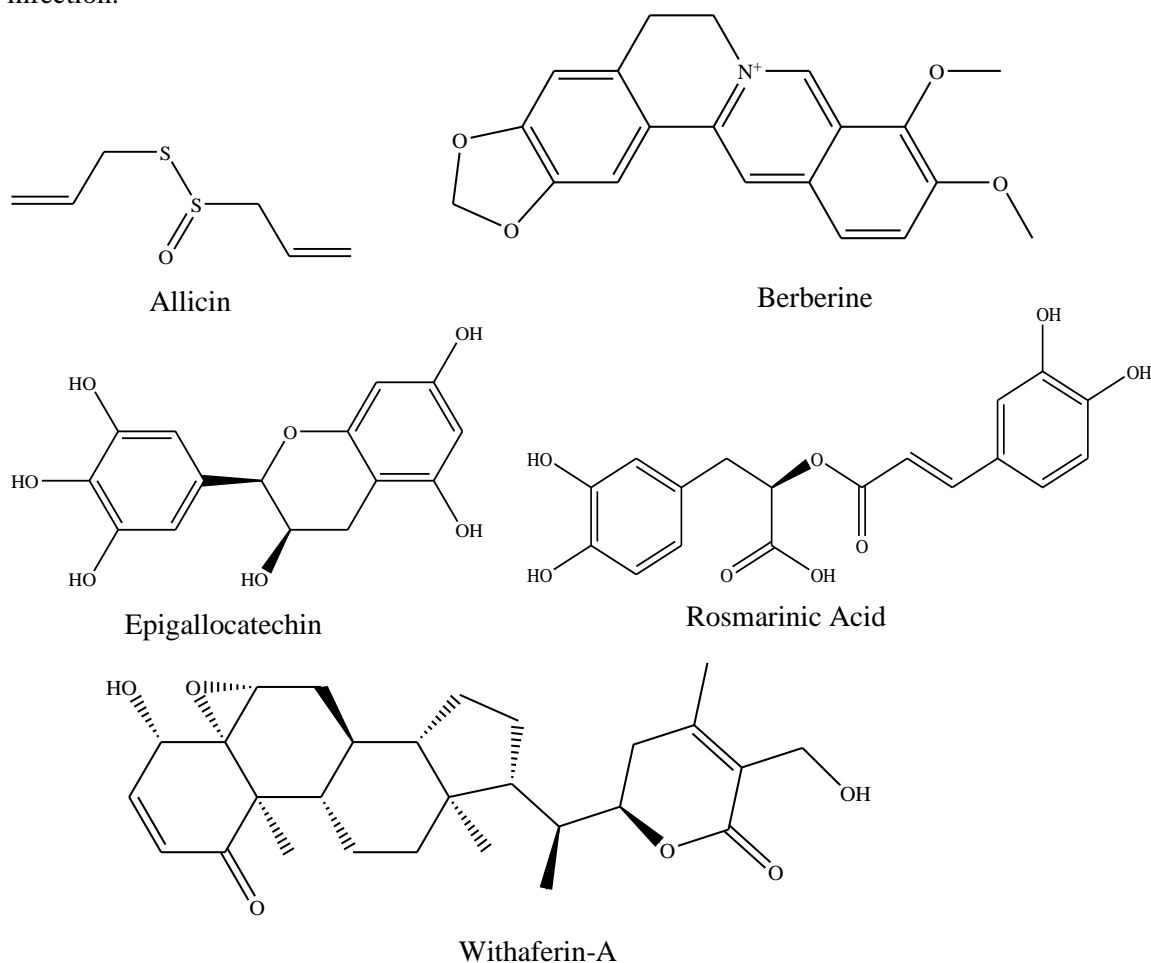


**Figure 1.** Structures of selected active constituents of natural products.

## 2. Experimental

### 2.1. Structure Retrieval and Binding Site

The three-dimension structures of ACE, IL-6, NADPH Oxidase, and TNF- $\alpha$  with PDB ID: 1O8A, 2CDU, 1ALU, and 2AZ5 were downloaded from research collaboratory in structural bioinformatics, protein data bank (RCSB, PDB) (<https://www.rcsb.org/>) with 2Å, 1.8Å, 1.9Å and 2.1Å resolution. Co-crystallized ligands were removed by BIOVIA discovery studio 2021. 3D structures of allicin, berberine, epigallocatechin, rosmarinic acid, and withaferin-A retrieved from NCBI Pubchem database (<https://pubchem.ncbi.nlm.nih.gov/>). The blind docking (BD) was performed where the entire surface of the protein is selected to recognize binding pockets of ligand.

### 2.2. Molecular Docking

Molecular docking was performed with the Autodock 4.2 software (The Scripps Research Institute, CA, USA) on four different minimized targets (ACE, IL-6, NADPH Oxidase, and TNF- $\alpha$ ) to evaluate docking poses of Allicin, Berberine, Epigallocatechin, Rosmarinic acid, and Withaferin-A. Polar hydrogen atoms were added and kolmann charges were added to protein using Autodock tools 1.5. Geister partial charges were added to the ligands and rotatable bonds were permitted to freely rotate

## Discovering the potential of natural remedies in the post COVID-19 complications

whereas the molecule was considered rigid.<sup>40</sup> The AutoGrid application was used to create 3D affinity grid fields. Both the grid and docking parameter files were generated using the AutoDock tools software (i.e., gpf and dpf). The docking parameters were set to 50 automated runs for a 300-population size, with a maximum number of energy evaluations of 2,500,000 for each docking experiment, and the search method was the Lamarckian genetic algorithm.<sup>41</sup> Ligplot+ v.2.2.4 was used to examine the interactions of docked complex protein-ligand conformations, comprising hydrogen bonds and bond lengths.<sup>42-44</sup>

### 2.3. Molecular Docking Simulation (MDS)

In order to further clarify the binding stability of the compound and elucidate the role of its side chain, standard MD simulations were performed with NAMD code ver. 2.9 on both ACE and TNF sequences. The parm99 Amber force field, including the recent nucleic acids parmbsc0 parameters was used. Complexes were then placed in a 12.0 Å layer cubic water box using the TIP3P explicit water model. K<sup>+</sup> cations were added to neutralize the net charge. The SHAKE algorithm was applied to constraint bonds involving hydrogen atoms. A 2 fs integration time step was considered. Ligand charges were computed using the restrained electrostatic potential (RESP) fitting procedure. The ESP was first calculated by means of Jaguar application ver. 8.3 using a 6-31G\* basis set at the Hartree-Fock level of theory. Finally, the RESP charges were calculated by means of the Antechamber module. The system was thus subjected to a double minimization step using the conjugate gradient algorithm in the following conditions: (i) minimization of water molecules and ions, keeping all the solute fixed (2000 steps); (ii) minimization of the entire system, without any restriction (2000 steps). The system was thus equilibrated at 300 K through 1ns in NVT and 1 atm through 1 ns in NPT ensembles before performing the MD production run of 50 ns in the NPT ensemble.

### 2.4. In-silico ADME Prediction for Some Active Natural Compounds

Using the pkcsm (<http://biosig.unimelb.edu.au/pkcsm/>) server, all docking structures were evaluated for in silico drug-likeness using Lipinski's law (Table 1). The program determines the compound's characteristics like Molecular Weight, Octanol-water partition coefficient, Surface area, Number of Hydrogen bond acceptors, Number of Hydrogen bond donors, and Violations from Lipinski's rule. It also predicts the effect of the ligand on ADME properties such as Water solubility (log mol/L), Caco2 permeability (log Papp in 10<sup>-6</sup> cm/s), Human intestinal absorption (% Absorbed), Skin permeability (log Kp), P-glycoprotein I inhibitor, P-glycoprotein II inhibitor, Human volume of distribution (log L/kg), Fraction unbound (human) (Fu), BBB permeability (logBB), CNS permeability (log PS), CYP3A4 inhibitor, CYP2C9 inhibitor, Total clearance (log mL/min/kg), Renal OCT2 (organic cation transporter 2) substrate, AMES toxicity, maximum recommended tolerated dose (human, log mg/kg/day), hERG I inhibitor, hERG II inhibitor, oral rat acute toxicity (LD50, mol/kg), oral rat chronic toxicity (lowest dose of a compound that results in an observed adverse effect (LOAEL), log mg/ kg bw/day), hepatotoxicity, skin sensitization, T. Pyriformis toxicity (log µg/L), minnow toxicity (log mM).

## 3. Results and Discussion

### 3.1. Molecular Docking

This study utilizes molecular docking to better understand the interactions of natural products with post COVID-19 causing targets such ACE, IL-6, NADPH Oxidase, and TNF- $\alpha$ . Target selection is an important aspect of the docking process, and all of these targets are to some extent responsible for post COVID-19 problems. The benefit of blind docking is to identify allosteric binding sites or exosites.<sup>45</sup> Following a thorough review of the literature, we discovered a few natural substances that can bind to these targets and may be effective in the treatment of post COVID-19 problems. The docking technique was followed step by step, and the output was in DLG form (Autodock docking log file). The RMSD (Root Mean Square Deviation), binding energy, Ki (Inhibition Constant), number of hydrogen bonds, and amino acid interactions are all listed in the results table.

**Table 1.** Molecular docking score of ligands against different proteins and hydrogen bonding interaction

| Compound         | Protein | RMSD (Å) | Binding energy (kcal/mol) | Inhibition constant (Ki) | No. of H bonds (ligand-protein) | Amino acid involved in interaction   |
|------------------|---------|----------|---------------------------|--------------------------|---------------------------------|--|
| Allicin          |         | 64.37    | -5.27                     | 136.74 uM                | 1                               | Leu161(A)  |
| Berberine        |         | 77.73    | -7.76                     | 02.05 uM                 | 1                               | Gly404(A)  |
| Epigallocatechin |         | 79.10    | -6.04                     | 37.62 uM                 | 6                               | Asp121(A),<br>Tyr213(A),<br>Ser222(A),<br>Glu403(A)                            |
| Rosmarinic acid  | ACE     | 79.57    | -6.47                     | 18.11 uM                 | 8                               | Asn68(A),<br>Ser339(A),<br>Glu342(A),<br>Thr345(A),<br>Asp346(A),<br>Arg348(A) |
| Withaferin-A     |         | 77.39    | -11.26                    | 05.58 nM                 | 3                               | Asn66(A),<br>Asn85(A),<br>Asp358(A)  |
| Allicin          |         | 31.07    | -4.18                     | 861.44 uM                | 1                               | Thr163(A)  |
| Berberine        |         | 13.27    | -6.80                     | 10.39 uM                 | 1                               | Gln175(A)  |
| Epigallocatechin |         | 29.74    | -6.59                     | 14.80 uM                 | 3                               | Leu64(A),<br>Lys86(A),<br>Glu93(A)   |
| Rosmarinic acid  | IL-6    | 11.04    | -7.63                     | 02.56 uM                 | 6                               | Asp26(A),<br>Arg30(A),<br>Asp34(A),<br>Arg179(A),<br>Arg182(A)                 |
| Withaferin-A     |         | 38.38    | -8.80                     | 355.04 nM                | 4                               | Asn61(A),<br>Lys66(A),<br>Met67(A)   |
| Allicin          |         | 10.98    | -4.37                     | 627.20 uM                | 1                               | Val81(A)   |
| Berberine        |         | 03.57    | -7.93                     | 01.55 uM                 | 1                               | Ala11(A)   |
| Epigallocatechin |         | 10.74    | -8.36                     | 747.77 nM                | 5                               | Ala45(A),<br>Glu163(A),<br>Gly329(A),<br>Gln426(B)                             |
| Rosmarinic acid  | NADPH   | 6.07     | -5.90                     | 47.22 uM                 | 6                               | Asn34(A),<br>Asn36(A),<br>Ser41(A),<br>Lys134(A),<br>Tyr136(A),<br>Ala300(A)   |
| Withaferin-A     |         | 53.13    | -9.43                     | 121.81 nM                | 6                               | Thr118(B),<br>Ile160(B),<br>Tyr159(B),<br>Phe245(B),<br>Asn261(B)              |

## Discovering the potential of natural remedies in the post COVID-19 complications

Table 1 continued..

|                                   |        |       |           |   |   |
|-----------------------------------|--------|-------|-----------|---|---|
| Allicin                           | 91.69  | -5.19 | 156.13 uM | 2 | Arg32(B),<br>Gly148(B)                            |
| Berberine                         | 80.02  | -7.20 | 05.25 uM  | 1 | Tyr151(B)   |
| Epigallocatechin<br>TNF- $\alpha$ | 71.20  | -6.85 | 09.50 uM  | 5 | Asp10(B),<br>Lys11(B),<br>Leu157(A),<br>Leu157(B) |
| Rosmarinic acid                   | 100.93 | -6.00 | 40.10 uM  | 4 | Arg103(B),<br>Lys112(B)                           |
| Withaferin-A                      | 83.89  | -8.54 | 551.90 nM | 3 | Ser60(B),<br>Pro117(B),<br>Tyr119(B)              |

The binding energies of all active ingredients of natural products and their derivatives to ACE, IL-6, NADPH Oxidase, and TNF-  $\alpha$  (binding energies ranging from  $-11.26$  to  $-4.18$  kcal/mol) are listed in Table 1. Furthermore, visual inspection of the computationally docked optimal binding poses of all NPs on all four proteins indicated the importance of several types of interactions, including hydrogen bonding and hydrophobic interactions.

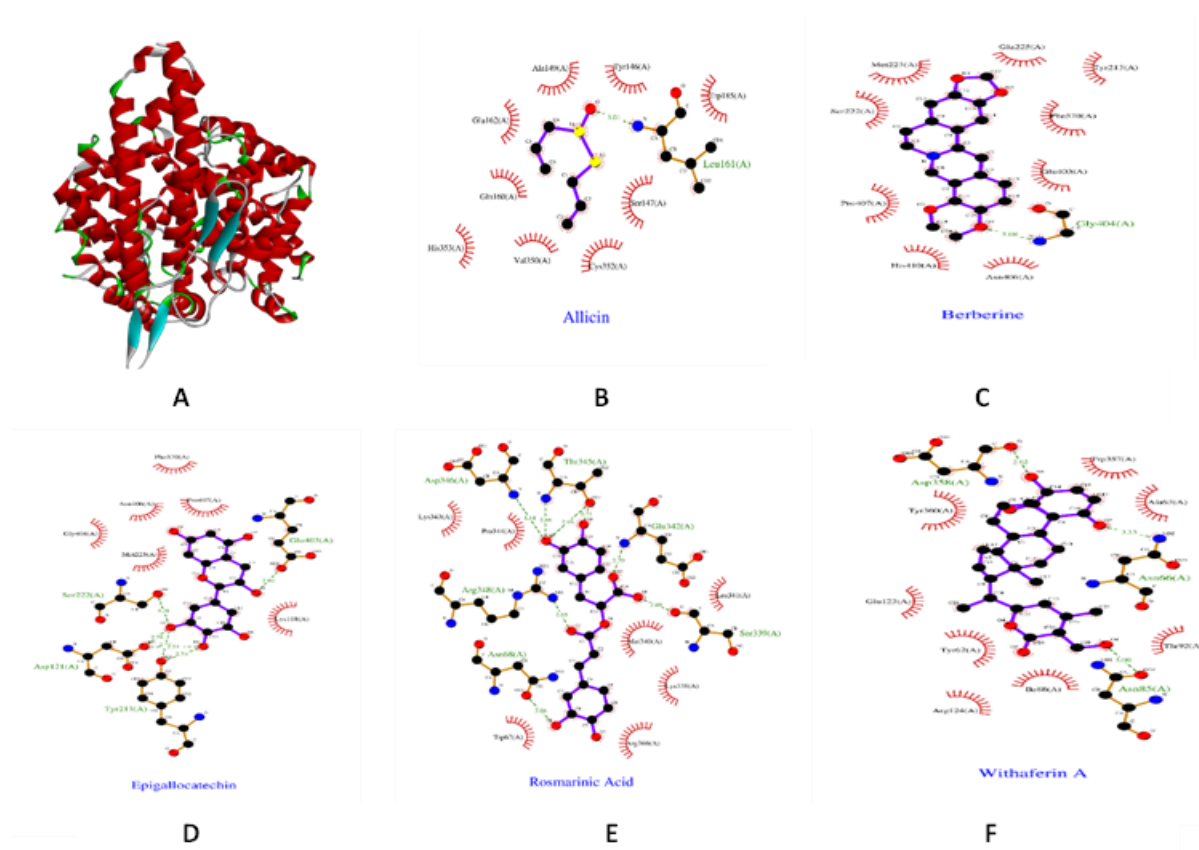


**Figure 2.** A: Crystal structure of ACH; B-F: Interaction of natural compounds with ACH

Among five natural compounds, Withaferin-A shows the lowest binding energy with all four proteins while Berberine, Epigallocatechin, and Rosmarinic acid 's binding energies varied from protein

to protein whereas Allicin has the least binding energy with all four proteins. Withaferin-A and Berberine bind efficiently to the ACE, with the binding energy of -11.26 and -7.76 kcal/mol, and three (Figure 2F) and one hydrogen bond(s) (Figure 2C) respectively. Withaferin-A and Rosmarinic acid have bind effectively with -8.80 and -7.63 kcal/mol and four (Figure 3F) and six (Figure 3E) hydrogen bond interactions. For NADPH Withaferin-A and Epigallocatechin (-9.43, -7.93 kcal/mol with six (Figure 4F) and one (Figure 4D) hydrogen bonds respectively) while for TNF- $\alpha$  Withaferin-A and Berberine were found with low binding energy. (-8.54, -7.20 kcal/mol with three (Figure 5F) and one (Figure 5B) hydrogen bond(s) respectively). In terms of hydrogen bond interaction Rosmarinic acid has formed highest eight hydrogen bonds (Asn68(A), Ser339(A), Glu342(A), Thr345(A), Asp346(A), Arg348(A); BE:-6.47; Figure 2E) with ACE, six bonds with IL-6 (Asp26(A), Arg30(A), Asp34(A), Arg179(A), Arg182(A); BE:-7.63; Figure 3E) and six with NADPH (Asn34(A), Asn36(A), Ser41(A), Lys134(A), Tyr136(A), Ala300(A)) whereas Berberine shows highest (Five) hydrogen bond interaction with TNF- $\alpha$  (Asp10(B), Lys11(B), Leu157(A),Leu157(B);Figure 5C). With different proteins, all of the chemicals have diverse bonding and nonbonding interactions. Our most notable molecule, Withaferin A, exhibits alkyl and pi-alkyl interactions with Ile88, Arg124, and Ala125, and even a hydrogen bond with ACE. Van der Waals and alkyl interactions were observed on IL6 with Leu62, Leu64, Leu135, Ser163, and Arg168. Van der Waals and Alkyl, Pi-Alkyl interactions were produced with Leu297, Leu299, Pro298 and other amino acids with NADPH, and the same type of interaction occurred with ACE with different amino acids.

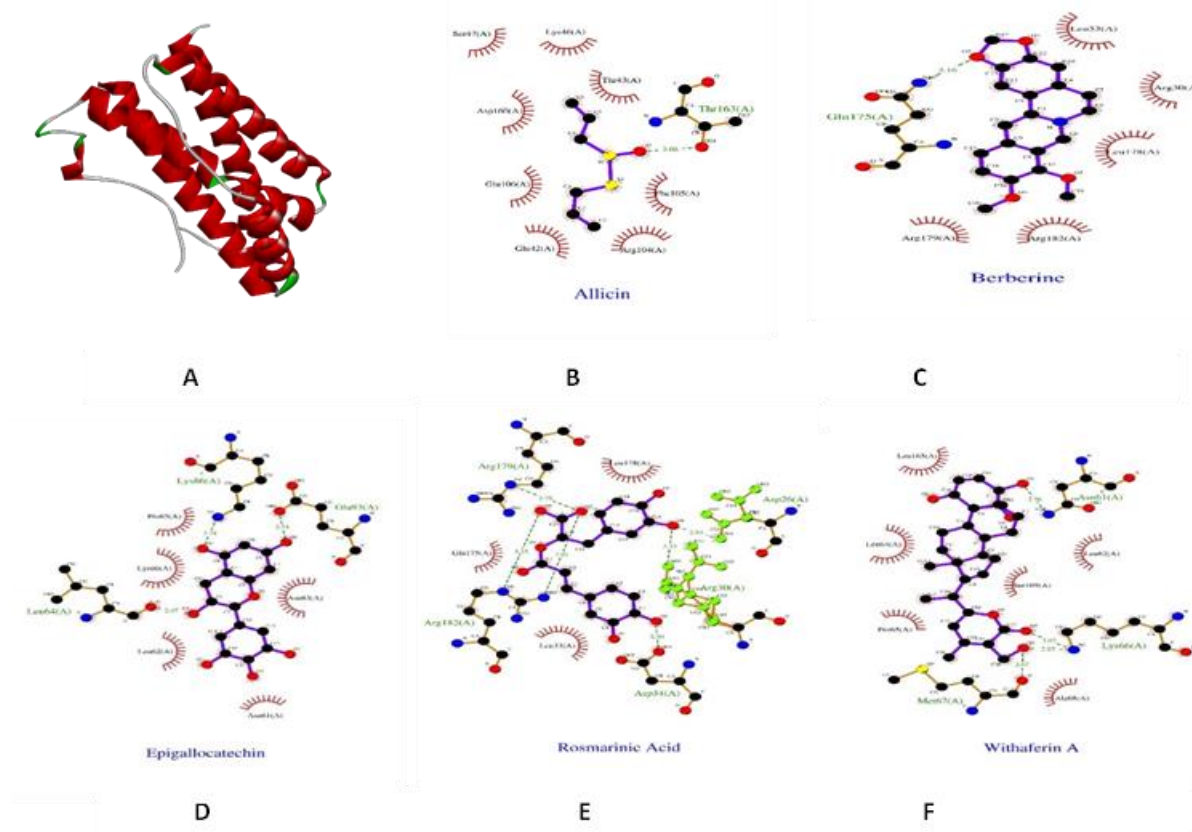


**Figure 3. A:** Crystal structure of IL-6; **B-F:** Interaction of natural compounds with IL-6.



## Discovering the potential of natural remedies in the post COVID-19 complications

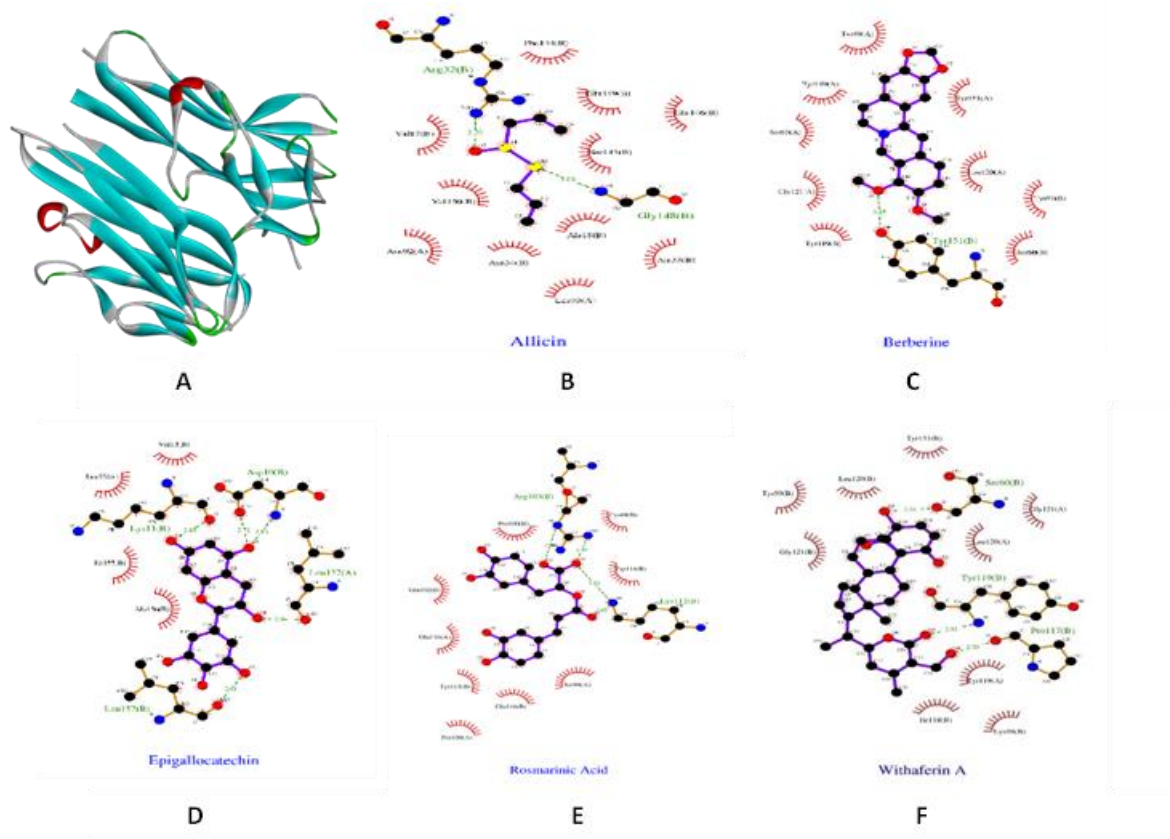


**Figure 4.** A: Crystal structure of NADPH; B-F: Interaction of natural compounds with NADPH.

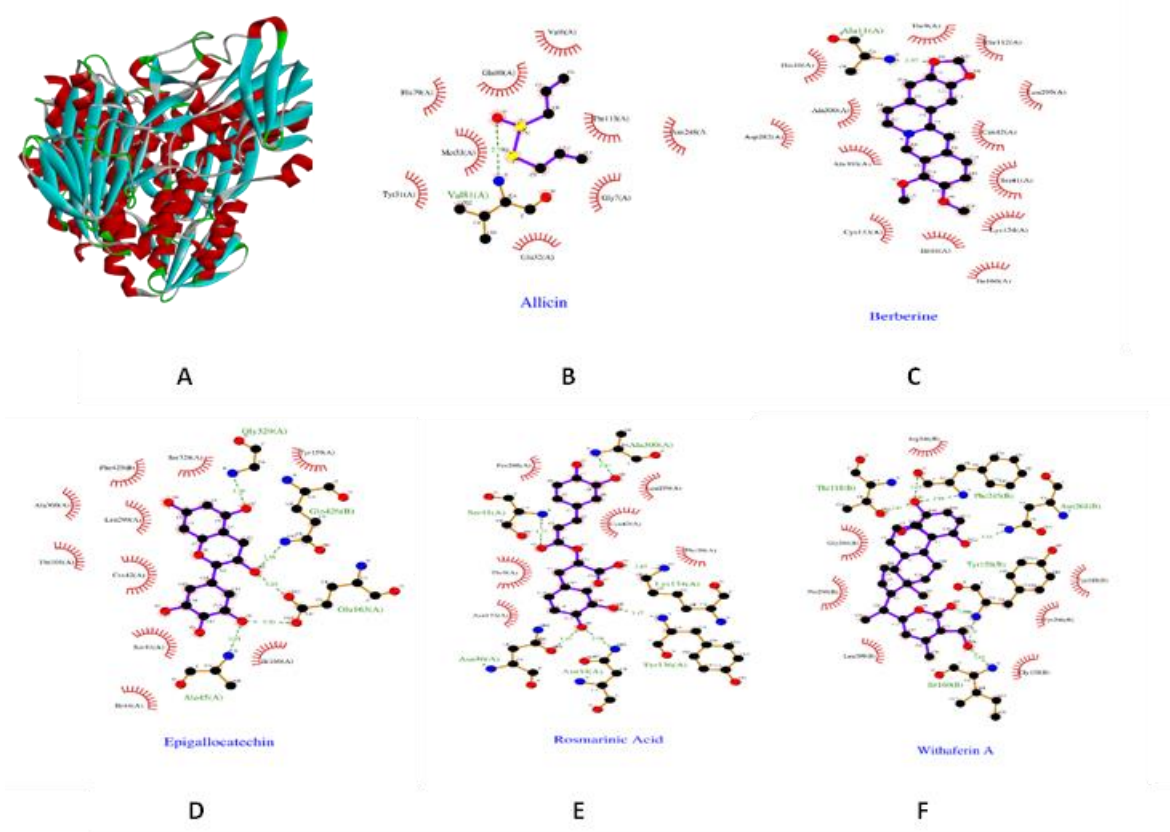


**Figure 5.** A: Crystal structure of TNF- $\alpha$ ; B-F: Interaction of natural compounds with TNF- $\alpha$ .

### 3.2 Molecular Docking Simulation

With the aim to explain the binding stability of our reference compound and to clarify the role of its side chain, molecular dynamics simulations (MDs) were performed using NAMD program with the parameters reported in the experimental section. After 50 ns of MDs of human angiotensin converting enzyme (Human ACE) complex and Tumour Necrosis factor- $\alpha$  (TNF- $\alpha$ ) complexes, the ligand was found to stabilize the G4 core without unfolded structure. Specifically, the Root Mean Square deviation (RMSd) calculated on the guanines core showed the slightly lower average value (equal to 1.20 Å) for the human angiotensin converting enzyme (Human ACE) complex, with respect to that of Tumour Necrosis factor- $\alpha$  (TNF- $\alpha$ ) complexes (RMSd equal to 1.37 Å).

Moreover, to better characterize the interactions between the ligand and both G4 receptors, we evaluated the non-bonded interaction energies in terms of electrostatic and Van der Waal's single contributions, using the NAMD Energy Plugin. We observed that, according to the theoretical docking data, the average Interaction Energy value, calculated after 50 ns of MDs, was equal to  $-84.12$  kcal/mol and  $-95.32$  kcal/mol for human angiotensin converting enzyme (Human ACE) complex and Tumour Necrosis factor- $\alpha$  (TNF- $\alpha$ ) complexes respectively. In particular, it was evident that in ACE complex, after approximately 25 ns, the Van der Waal's term was associated to the major contribution, accordingly to a sandwiched binding mode between the berberine core and with 2-acetamido-2-deoxy-beta-D-glucopyranose respectively. Conversely, for the Tumour Necrosis factor- $\alpha$  (TNF- $\alpha$ ) complexes, the electrostatic and Van der Waal's energetic contributions were almost equivalent (Figure 7 A and B).

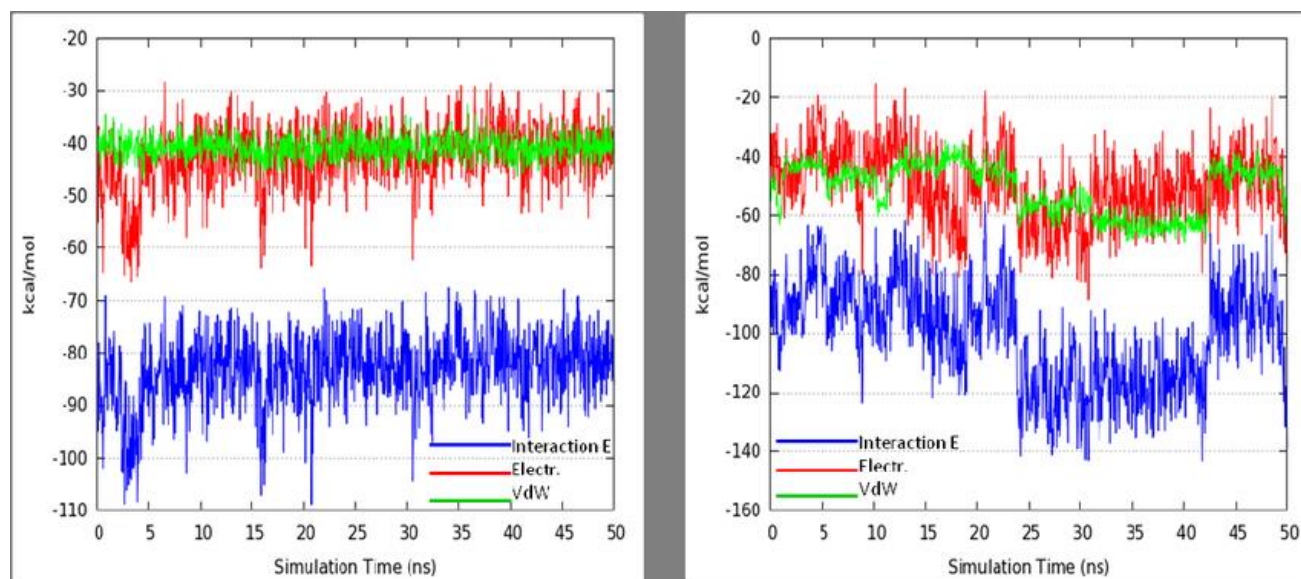


**Figure 6.** MD simulation of Berberine for ACE (a-left side) and TNF- $\alpha$  (b- right side)

### 3.3 In-silico Drug-likeness and Pharmacokinetic Property Prediction

Natural materials utilized in this study have MW values ( $MW < 500$ ) required for efficient penetration across biological membranes. The predicted lipophilicity (given as LogP) for all of the compounds was found to be significantly higher than the standard cut-off value of 5 employed in drug design. The surface area (SA) range for all components was determined to be 62.082 – 201.3172, which is well within the limit.

## Discovering the potential of natural remedies in the post COVID-19 complications

**Table 2.** In-silico prediction of drug-likeness for some active natural compounds

| Compound         | MW      | LogP   | SA      | HBA | HBD | n violations | Rotatable Bonds |
|------------------|---------|--------|---------|-----|-----|--------------|-----------------|
| Allicin          | 162.279 | 1.7553 | 62.082  | 2   | 0   | 0            | 5               |
| Berberine        | 336.367 | 3.0963 | 144.867 | 4   | 0   | 0            | 2               |
| Epigallocatechin | 306.27  | 1.2517 | 124.456 | 7   | 6   | 1            | 1               |
| Rosmarinic Acid  | 360.318 | 1.7613 | 147.396 | 7   | 5   | 0            | 6               |
| Withaferin A     | 470.606 | 3.3529 | 201.317 | 6   | 2   | 0            | 3               |

MW: Molecular Weight; LogP: Octanol-water partition coefficient; SA: Surface area; HBA: Number of Hydrogen bond acceptor; HBD: Number of Hydrogen bond donor; n violations: Violations from Lipinski's rule.

In addition, the pkCSM server was used to determine numerous critical ADMET (Absorption, Distribution, Metabolism, Excretion, and Toxicity) characteristics. The findings are shown in Tables 3. The water solubility of all-natural components was moderate to high, ranging from -2.969 log mol/L (Epigallocatechin) to -5.063 log mol/L (Withaferin A). Except for Withaferin A (permeation= 0.829), Rosmarinic Acid (permeation= -0.937), and Epigallocatechin (permeation= -2.969), all substances had significant Caco-2 permeability (permeation > 0.90). Except for Rosmarinic Acid (Intestinal permeability = 32.516 %) and Epigallocatechin (Intestinal permeability = 54.128 %), all-natural substances exhibited Intestinal permeability of more than 85 %, suggesting excellent permeability through the intestinal membrane. Except for Allicin (skin permeability = -1.877), all-natural components demonstrated high skin permeability (Permeation > -2.5). Except for Withaferin A, no natural components inhibited P-glycoprotein I. Except for Withaferin A and Berberine, no natural components inhibited P-glycoprotein II. Moreover, except for Rosmarinic Acid and Epigallocatechin, all NPs had low BBB permeability and moderate CNS permeability. The metabolizing enzyme CYP3A4 was not inhibited by any of the natural components. Except for Berberine, no natural components inhibited the metabolizing enzyme CYP2C9. The overall clearance of all Natural components derivatives was found to be in the range of 0.25 log mL/min/kg (Rosmarinic Acid) to 1.27 log mL/min/kg (Rosmarinic acid). Except for Withaferin A, all Natural components were discovered to be OCT2 substrates, indicating that these drugs will have no adverse interactions and will have no detrimental effect on renal clearance

According to the toxicity results except for Berberine, which has exhibited AMES toxicity, other selected natural compounds do not show AMES toxicity. All drugs have a maximum tolerable dose of -0.695 (Withaferin A) to 0.737 (Allicin) log mg/kg/day. None of them are inhibitors of hERG I or hERG II. Berberine has the tendency to create hepatotoxicity, whereas allicin has the possibility to trigger skin hypersensitivity. The toxicity of T.Pyriformis and Minnow was in the range of 0.299 (Withaferin A) to 0.9 (Allicin) and -0.277 (Berberine) to 4.235 (Epigallocatechin), respectively.

All molecules fall within the allowed range, indicating that the proposed molecule has a high bioavailability. The number of hydrogen bond acceptors ( $HBA \leq 10$ ) and donors ( $HBD \leq 5$ ) for all compounds followed Lipinski's rule of five. In any of the natural compounds, there is no nviolation. Rosmarinic Acid has the most rotatable bonds - 6, followed by Allicin - 5, Withaferin A -3, Berberine -2, and epigallocatechin -1 rotatable bond(s).

**Table 3.** In-silico ADME prediction for some active natural compounds

| Compound         | Absorption |        |        |        | Distribution |      |        | Metabolism |       | Excretion |      |      |       |     |
|------------------|------------|--------|--------|--------|--------------|------|--------|------------|-------|-----------|------|------|-------|-----|
|                  | WS         | CP     | IA     | SP     | PI-1         | PI-2 | VD     | FU         | BBB   | CNS       | CI-1 | CI-2 | TC    | RS  |
| Allicin          | -1.72      | 1.316  | 96.229 | -1.877 | No           | No   | -0.045 | 0.577      | 0.506 | -2.312    | No   | No   | 0.714 | No  |
| Berberine        | -3.973     | 1.734  | 97.147 | -2.576 | No           | Yes  | 0.58   | 0.262      | 0.198 | -1.543    | No   | Yes  | 1.27  | No  |
| Epigallocatechin | -2.969     | -0.375 | 54.128 | -2.735 | No           | No   | 1.301  | 0.274      | -     | -3.507    | No   | No   | 0.328 | No  |
| Rosmarinic Acid  | -3.059     | -0.937 | 32.516 | -2.735 | No           | No   | 0.393  | 0.348      | -     | -3.347    | No   | No   | 0.25  | No  |
| Withaferin A     | -5.063     | 0.829  | 85.345 | -3.202 | Yes          | Yes  | -0.131 | 0.105      | -0.03 | -2.72     | No   | No   | 0.435 | Yes |

WS – Water solubility (log mol/L), CP – Caco2 permeability (log Papp in 10<sup>-6</sup> cm/s), IA – Human intestinal absorption (% Absorbed), SP – Skin permeability (log Kp), PI-1 – P-glycoprotein I inhibitor, PI-2 – P-glycoprotein II inhibitor, VD – Human volume of distribution (log L/kg), FU – Fraction unbound (human) (Fu), BBB – BBB permeability (logBB), CNS – CNS permeability (log PS), CI-1 – CYP3A4 inhibitor, CI-2 – CYP2C9 inhibitor, TC – Total clearance (log mL/min/kg), RS – Renal OCT2 (organic cation transporter 2) substrate.

**Table 4.** In-silico TOXICITY prediction for some active natural compounds

| Compound         | AT  | MRTD   | hERGI | hERGII | ORAT  | ORCT  | HT  | SS  | TPT   | MT     |
|------------------|-----|--------|-------|--------|-------|-------|-----|-----|-------|--------|
| Allicin          | No  | 0.737  | No    | No     | 2.366 | 1.406 | No  | Yes | 0.9   | 1.235  |
| Berberine        | Yes | 0.144  | No    | No     | 2.571 | 1.89  | Yes | No  | 0.354 | -0.277 |
| Epigallocatechin | No  | 0.506  | No    | No     | 2.492 | 2.927 | No  | No  | 0.286 | 4.235  |
| Rosmarinic Acid  | No  | 0.152  | No    | No     | 2.811 | 2.907 | No  | No  | 0.302 | 2.698  |
| Withaferin A     | No  | -0.695 | No    | No     | 2.779 | 0.918 | No  | No  | 0.299 | 0.738  |

AT – AMES toxicity, MRTD– maximum recommended tolerated dose (human, log mg/kg/day), hERGI - hERG I inhibitor, hERGII – hERG II inhibitor, ORAT-oral rat acute toxicity (LD50, mol/kg), ORCT-oral rat chronic toxicity (lowest dose of a compound that results in an observed adverse effect (LOAEL), log mg/ kg bw/day), HT-hepatotoxicity, SS- skin sensitization, TPT-T.Pyriformis toxicity (log µg/L), MT-minnow toxicity (log mM).

#### 4. Conclusion

COVID-19 impact made major challenges in the people life and healthcare sector. During infection tremendous tissue injuries observed in lungs, pancreas, liver and kidneys with surge in multiple inflammatory cytokines. There are many symptoms which are remains after disappearance of virus and its products from the human body that can be considered as post COVID-19 syndrome. Patients with already suffering from respiratory, renal and endocrine system disorders seem more vulnerable. Vaccine and available therapeutic modalities seem insufficient to work under this situation. Based on available literature we searched for potent phytoconstituents from natural origin and main targets which are responsible for post COVID-19 complication. Many herbs shown excellent outcome in slow the progression and severity of the disease. Further we have carried out docking to validate the data with auto dock. According to the in-silico data, Withaferin-A is the most efficient herbal constituent, with a higher tendency to bind ACE, IL-6, NADPH, and TNF- $\alpha$  than other natural substances. Berberine has shown higher score in MD simulation study compared to other phytoconstituents. To verify its efficacy even further, additional cell-line study and pre-clinical trials are needed.

#### Acknowledgements

We authors are thankful to Ramanbhai Patel college of Pharmacy, CHARUSAT, Gujarat, India for providing facilities to complete the work of this article.

#### ORCID

Alkeshkumar Patel: [0000-0001-7036-5011](https://orcid.org/0000-0001-7036-5011)

Ashish Patel: [0000-0001-5773-3756](https://orcid.org/0000-0001-5773-3756)

Rushikumar Shah: [0000-0002-1981-1909](https://orcid.org/0000-0002-1981-1909)

Diwyanshi Zinzuvadia: [0000-0003-3614-2732](https://orcid.org/0000-0003-3614-2732)

Sagar Mahant: [0000-0002-2022-324X](https://orcid.org/0000-0002-2022-324X)

#### References

- [1] Costela-Ruiz, V.J.; Illescas-Montes, R.; Puerta-Puerta, J.M.; Ruiz, C.; Melguizo-Rodríguez, L. SARS-CoV-2 infection: the role of cytokines in COVID-19 disease. *Cytokine Growth Factor Rev.* **2020**, *54*, 62-75.
- [2] Habas, K.; Nganwuchu, C.; Shahzad, F.; Gopalan, R.; Haque, M.; Rahman, S.; Mjumder, A.A.; Nasim, T. Resolution of coronavirus disease 2019 (COVID-19). *Expert Rev. Anti-Infect. Therap.* **2020**, *18* (12), 201-1211.
- [3] Soy, M.; Keser, G.; Atagündüz, P.; Tabak, F.; Atagündüz, I.; Kayhan, S. Cytokine storm in COVID-19: pathogenesis and overview of anti-inflammatory agents used in treatment. *Clin. Rheumatol.* **2020**, *39* (7), 2085-2094.
- [4] Umakanthan, S.; Sahu, P.; Ranade, A. V.; Bukelo, M.M.; Sushil, R.; Abrahao-Machado, L.F.; Dahal, S.; Kumar, H.; Kv, D. Origin, transmission, diagnosis and management of coronavirus disease 2019 (COVID-19). *Postgrad. Medical J.* **2020**, *96* (1142), 753-758.

- [5] Cascella, M.; Rajnik, M.; Aleem, A.; Dulebohn, S.C.; Di Napoli, R. Features, Evaluation, and treatment of coronavirus-StatPearls-NCBIBookshelf. Published online **2021**. <https://www.ncbi.nlm.nih.gov/books/NBK554776/>
- [6] Chen, J.; Wang, R.; Gilby, N.B.; Wei, G.W. Omicron (B.1.1.529): Infectivity, vaccine breakthrough, and antibody resistance. Published online December 1, **2021**. <http://arxiv.org/abs/2112.01318>
- [7] Gavriatopoulou, M.; Ntanas-Stathopoulos, I.; Korompoki, E.; Ftiou, M.; Tzanninis, I.G.; Psaltopoulou, T.; Kastiris, E.; Terpos, E.; Dimopoulou, M.A. Emerging treatment strategies for COVID-19 infection. *Clin. Experiment. Medicin.* **2021**, *21*(2), 167-179.
- [8] Chakraborty, S.; Mallajosyula, V.; Tato, C.M.; Tan, G.S.; Wang, T.T. SARS-CoV-2 vaccines in advanced clinical trials: where do we stand? *Adv. Drug Deliv. Rev.* **2021**, *172*, 314-338.
- [9] Bakhiet, M.; Taurin, S. SARS-CoV-2: Targeted managements and vaccine development. *Cytokine Growth Factor Rev.* **2021**, *58*, 16-29.
- [10] Francis, A.I.; Ghany, S.; Gilkes, T.; Umakanthan, S. Review of COVID-19 vaccine subtypes, efficacy and geographical distributions. *Postgrad. Medical J.* Published online **2021**, 140654.doi:10.1136/postgradmedj-2021-140654
- [11] Agarwal, S.; Saha, S.; Darbar, S. COVID-19 Vaccine: COVAXIN®-India's first indigenous effective weapon to fight against Coronavirus (A Review). *Parana J. Sci. Education.* **2021**, *7*(3), 1-9.
- [12] Nalbandian, A.; Sehgal, K.; Gupta, A.; Madhavan, M.V.; McGroder, C.; Stevens, J.S.; Cook, J.R.; Nordvig, A.S.; Shalev, D.; Sehwat, T.S. et al. Post-acute COVID-19 syndrome. *Nature Medicine.* **2021**, *27*(4), 601-615.
- [13] Mahmud, R.; Rahman, M.M.; Rassel, M.A.; Monayem, F.B.; Sayeed, S.J.; Islam, M.S.; Islam, M.M. Post-COVID-19 syndrome among symptomatic COVID-19 patients: A prospective cohort study in a tertiary care center of Bangladesh. *PloS One* **2021**, *16*(4), 1-13.
- [14] Pavoni, V.; Giancesello, L.; Pazzi, M.; Stera, C.; Meconi, T.; Frigieri, F.C. Evaluation of coagulation function by rotation thromboelastometry in critically ill patients with severe COVID-19 pneumonia. *J. Thromb. Thrombolysis.* **2020**, *50*(2), 281-286.
- [15] Jiang, L.; Tang, K.; Levin, M.; Irfan, O.; Morris, S.K.; Wilson, K.; Klein, J.D.; Bhutta, Z.A. COVID-19 and multisystem inflammatory syndrome in children and adolescents. *Lancet Infect. Dis.* **2020**, *20*(11), e276-e288.
- [16] Tang, X.; Uhl, S.; Zhang, T.; Xue, D.; Li, B.; Vandana, J.J.; Acklin, J.A.; Bonnycastle, L.L.; Narisu, N.; Erdos, M.R. et al. SARS-CoV-2 infection induces beta cell transdifferentiation. *Cell Metab.* **2021**, *33*(8), 1577-1591.e7.
- [17] Suvvari, T.K.; Kutikuppala, L.V.S.; Tsagkaris, C.; Corriero, A.C.; Kandi, V. Post-COVID-19 complications: Multisystemic approach. *J. Med. Virol.* **2021**, *93*, 6451-6455.
- [18] McElvaney, O.J.; McEvoy, N.L.; McElvaney, O.F.; Carroll, T.P.; Murphy, M.P.; Dunlea, D.M.; Ní Choileáin, O.; Clarke, J.; O'Connor, E.; Hogan, G. et al. Characterization of the inflammatory response to severe COVID-19 illness. *Am. J. Respir. Crit. Care Med.* **2020**, *202*, 812-821.
- [19] Vihar, S.; Boushra, M.; Ntiamoah, P.; Biehl, M. Post-acute sequelae of SARS-CoV-2 infection: Caring for the 'long-haulers.' *Cleve. Clin. J. Med.* **2021**, *88*(5), 267-272.
- [20] Mrityunjaya, M.; Pavithra, V.; Neelam, R.; Janhavi, P.; Halami, P.M.; Ravindra, P.V. Immune-boosting, antioxidant and anti-inflammatory food supplements targeting pathogenesis of COVID-19. *Front. Immunol.* **2020**, *11*, 570122.
- [21] Name, J.J.; Souza, A.C.R.; Vasconcelos, A.R.; Prado, P.S.; Pereira, C.P.M. Zinc, Vitamin D and Vitamin C: Perspectives for COVID-19 with a focus on physical tissue barrier integrity. *Front. Nutr.* **2020**, *7*, 606398.
- [22] Saggam, A.; Limgaokar, K.; Borse, S.; Chavan-Gautam, P.; Dixit, S.; Tillu, G.; Patwardhan, B. *Withania somnifera* (L.) Dunal: Opportunity for clinical repurposing in COVID-19 management. *Front. Pharmacol.* **2021**, *12*, 623795.
- [23] Minhas, U.; Minz, R.; Das, P.; Bhatnagar, A. Therapeutic effect of *withania somnifera* on pristane-induced model of SLE. *Inflammopharmacology* **2012**, *20*(4), 195-205.
- [24] Jeyanthi, T.; Subramanian, P. Nephroprotective effect of *withania somnifera*: A dose-dependent study. *Ren Fail.* **2009**, *31*(9), 814-821.
- [25] Chukwuma, C.I.; Matsabisa, M.G.; Ibrahim, M.A.; Erukainure, O.L.; Chabalala, M.H.; Islam, M.S. Medicinal plants with concomitant anti-diabetic and anti-hypertensive effects as potential sources of dual acting therapies against diabetes and hypertension: A review. *J. Ethnopharmacol.* **2019**, *235*, 329-360.
- [26] Wang, Z.Z.; Li, K.; Maskey, A.R.; Huang, W.; Toutov, A.A.; Yang, N.; Srivastava, K.; Geliebter, J.; Tiwari, R.; Miao, M. et al. A small molecule compound berberine as an orally active therapeutic candidate against COVID-19 and SARS: A computational and mechanistic study. *FASEB J.* **2021**, *35*(4), e21360.
- [27] Varghese, F.S.; van Woudenberg, E.; Overheul, G.J.; Eleveld, M.J.; Kurver, L.; van Heerbeek, N.; van Laarhoven, A.; Miesen, P.; den Hartog, G.; de Jonge, M.I. et al. Berberine and obatoclax inhibit sars-cov-2 replication in primary human nasal epithelial cells in vitro. *Viruses* **2021**, *13*(2), 2132.

## Discovering the potential of natural remedies in the post COVID-19 complications

- [28] Mhatre, S.; Srivastava, T.; Naik, S.; Patravale, V. Antiviral activity of green tea and black tea polyphenols in prophylaxis and treatment of COVID-19: A review. *Phytomedicine* **2021**, *85*, 153286.
- [29] Chourasia, M.; Koppula, P.R.; Battu, A.; Ouseph, M.M.; Singh, A.K. EGCG, a green tea catechin, as a potential therapeutic agent for symptomatic and asymptomatic SARS-CoV-2 infection. *Molecules* **2021**, *26*(5), 1200 .
- [30] Nunes, S.; Madureira, A.R.; Campos, D.; Sarmento, B.; Gomes, A.M.; Pintado, M.; Reis, F. Therapeutic and nutraceutical potential of rosmarinic acid—Cytoprotective properties and pharmacokinetic profile. *Crit. Rev. Food Sci. Nutr.* **2017**, *57*(9), 1799-1806.
- [31] Ferreira, L.G.; Evora, P.R.B.; Capellini, V.K.; Albuquerque, A.A.; Carvalho, M.T.; da Silva Gomes, R.A.; Parolini, M.T.; Celotto, A.C. Effect of rosmarinic acid on the arterial blood pressure in normotensive and hypertensive rats: Role of ACE. *Phytomedicine* **2018**, *38*, 158-165.
- [32] Khalaf, A.A.; Hassanen, E.I.; Ibrahim, M.A.; Tohamy, A.F.; Aboseada, M.A.; Hassan, H.M.; Zaki, A.R. Rosmarinic acid attenuates chromium-induced hepatic and renal oxidative damage and DNA damage in rats. *J. Biochem.Mol. Toxicol.* **2020**, *34*(11), e22579.
- [33] Oguz, A.; Böyük, A.; Ekinci, A.; Alabalik, U.; Türkoğlu, A.; Tuncer, M.C.; Ekingen, A.; Deveci, E.; Gültürk, B.; Aday, U. Investigation of antioxidant effects of rosmarinic acid on liver, lung and kidney in rats: A biochemical and histopathological study. *Folia Morphol.* **2020**, *79*(2), 288-295.
- [34] Donma, M.M.; Donma, O. The effects of allium sativum on immunity within the scope of COVID-19 infection. *Med Hypothes.* **2020**, *144*, 109934
- [35] Shiravi, A.; Akbari, A.; Mohammadi, Z.; Khalilian, M.S.; Zeinalian, A.; Zeinalian, M. Rosemary and its protective potencies against COVID-19 and other cytokine storm associated infections: A molecular review. *Mediterranean. J. Nutr. Metabol.* **2021**, *14*, 401-416.
- [36] Herman, L.L.; Padala, S.A.; Annamaraju, P.B.K. Angiotensin converting enzyme inhibitors (ACEI). StatPearls Publishing; **2021**. <https://www.ncbi.nlm.nih.gov/books/NBK431051/>
- [37] Younus, H. Therapeutic potentials of superoxide dismutase. *Int. J. Health Sci.* **2018**, *12*(3), 88-93.
- [38] Laforge, M.; Elbim, C.; Frère, C.; Hémedi, M.; Massaad, C.; Nuss, P.; Benoliel, J.J.; Becker, C. Tissue damage from neutrophil-induced oxidative stress in COVID-19. *Nat Rev Immunol.* **2020**, *20*(9), 515-516.
- [39] Nigar, S.; Shah, S.T.; Setu, M.; Dip, S.D.; Ibnat, H.; Islam, M.T.; Akter, S.; Jahid, I.K.; Hossain, M.A. Relative expression of proinflammatory molecules in COVID-19 patients who manifested disease severities. *J. Med. Virol.* **2021**, *93* (10), 5805-5815.
- [40] Gasteiger, J.; Marsili, M. Iterative partial equalization of orbital electronegativity—a rapid access to atomic charges. *Tetrahedron* **1980**, *36* (22), 3219-3228.
- [41] Morris, G.M.; Goodsell, D.S.; Halliday, R.S.; Huey, R.; Hart, W.E.; Belew, R.K.; Olson, A.J. Automated docking using a Lamarckian genetic algorithm and an empirical binding free energy function. *J. Comput. Chem.* **1998**, *19*(14), 1639-1662.
- [42] Laskowski, R.A.; Swindells, M.B. LigPlot+: multiple ligand-protein interaction diagrams for drug discovery. *J. Chem. Inf. Model.* **2011**, *51*, 2778-2786.
- [43] Patel, A.; Patel, A.; Hemani, R.; Solanki, R.; Kansara, J.; Patel, G.; Pradhan, S.; Bambharoliya, T. Exploring the in-silico approach for assessing the potential of natural compounds as a SARS-CoV-2 main protease inhibitors. *Org. Commun.* **2021**, *14*(1), 58-72.
- [44] Patel, A.; Rajendran, M.; Shah, A.; Patel, H.; Pakala, S.B.; Karyala, P. Virtual screening of curcumin and its analogs against the spike surface glycoprotein of SARS-CoV-2 and SARS-CoV. *J. Biomol. Struct. Dyn.* **2020**, 1-9. doi: 10.1080/07391102.2020.1868338
- [45] Hetényi, C.; van der Spoel, D. Toward prediction of functional protein pockets using blind docking and pocket search algorithms. *Protein Sci.* **2011**, *20*(5), 880-893.

**A C G**  
publications

© 2022 ACG Publications